

Real-Time Applicability of Emulated Virtual Circuits for Tokamak Plasma Shape Control

Pedro Cavestany
*STFC Hartree Centre
 SciTech Daresbury*
 Warrington,
 WA4 4AD, UK

pedro.cavestany-olivares@stfc.ac.uk

Nicola C. Amorisco
UK Atomic Energy Authority
 Culham Campus, Abingdon,
 Oxfordshire,
 OX14 3DB, UK

nicola.amorisco@ukaea.uk

Alasdair Ross
*STFC Hartree Centre
 SciTech Daresbury*
 Warrington,
 WA4 4AD, UK

alasdair.ross@stfc.ac.uk

George K. Holt
*STFC Hartree Centre
 SciTech Daresbury*
 Warrington,
 WA4 4AD, UK

ORCID 0000-0001-6814-9117

Adriano Agnello
*STFC Hartree Centre
 SciTech Daresbury*
 Warrington,
 WA4 4AD, UK

ORCID 0000-0001-9775-0331

Aran Garrod
*STFC Hartree Centre
 SciTech Daresbury*
 Warrington,
 WA4 4AD, UK

aran.garrod@stfc.ac.uk

Kamran Pentland
UK Atomic Energy Authority
 Culham Campus, Abingdon,
 Oxfordshire,
 OX14 3DB, UK

James Buchanan
UK Atomic Energy Authority
 Culham Campus, Abingdon,
 Oxfordshire,
 OX14 3DB, UK

kamran.pentland@ukaea.uk

ORCID 0009-0009-0743-7655

Abstract—Machine learning has recently been adopted to emulate sensitivity matrices for real-time magnetic control of tokamak plasmas. However, these approaches would benefit from a quantification of possible inaccuracies. We report on two aspects of real-time applicability of emulators. First, we quantify the agreement of target displacement from VCs computed via Jacobians of the shape emulators with those from finite differences Jacobians on exact Grad-Shafranov solutions. Good agreement ($\approx 5\text{--}10\%$) can be achieved on a selection of geometric targets using combinations of neural network emulators with $\approx 10^5$ parameters. A sample of $\approx 10^5\text{--}10^6$ synthetic equilibria is essential to train emulators that are not over-regularised or overfitting. Smaller models trained on the shape targets may be further fine-tuned to better fit the Jacobians. Second, we address the effect of vessel currents that are not directly measured in real-time and are typically subsumed into effective “shaping currents” when designing virtual circuits. We demonstrate that shaping currents can be inferred via simple linear regression on a trailing window of active coil current measurements with residuals of only a few Ampères, enabling a choice for the most appropriate shaping currents at any point in a shot. While these results are based on historic shot data and simulations tailored to MAST-U, they indicate that emulators with few-millisecond latency can be developed for robust real-time plasma shape control in existing and upcoming tokamaks.

I. INTRODUCTION

One core task in magnetic confinement fusion with tokamaks is the control of the plasma position and shape, to maintain configurations with desirable confinement properties. This often amounts to the real-time control of a few geometric targets related to the boundary of the plasma [under a toroidal symmetry approximation, 1, 2, 3]. The plasma is shaped by magnetic fields from surrounding poloidal field (PF) coils, which must also compensate for the “stray”

varying magnetic field from Ohmic coils that are used to drive a plasma current. Typically, feed-forward sequences of desired target values are pre-computed, and control loops are designed to correct for any departure of the plasma control targets, on sub-millisecond timescales [5]. The configuration of the plasma is established on faster (1–10 μs) timescales and can be described by equilibrium solutions that satisfy the Grad–Shafranov (GS) equation. For each equilibrium, a sensitivity matrix can be computed as a Jacobian of the shape targets of interest with respect to the PF coil currents. Its pseudo-inverse then provides a set of *virtual circuits* (VCs), i.e. linear combinations of PF coil current changes that would correspond to independent changes in one shape target at a time. This is the approach commonly followed in classical shape control, where the plasma control system issues voltage requests to the power supplies to attain desired PF current changes to correct a departure between the desired and observed shape targets.

Approaches from machine learning have been recently proposed in the literature. Reinforcement learning (RL) can directly propose the voltage requests without any linearisation assumption [6, 7, 8], and the RL agents are trained on purely simulated environments or using information from experimental campaigns. Compared to classical control, RL has the advantage that resulting control policies can compensate for any effect that can be explicitly modelled in the training environment, e.g. currents induced in other metals in the vessel, which are not obvious to implement in classical control. The generalisation and explainability of RL in plasma shape control, however, remain an open problem [9].

While the classical approach with virtual circuits only requires Jacobians to be computed around configurations of interest, different configurations correspond to different

Jacobians and typically only a few are pre-computed for every experiment, hindering the robustness of control against non-negligible displacements.

Machine learning emulation can generalise the classical-control approach by providing target Jacobians at every time step of any foreseen experiment with very low latency. It also enables better explainability than RL as the remainder of the control loops are driven by a small number of parameters that can be tuned by the operators. Data-driven emulation of plasma shape has been developed for some tokamaks with long histories of campaigns [10] and also for data-sets that are built entirely on synthetic libraries of GS solutions [11].

This work examines two aspects of emulated virtual circuits that affect their applicability in real-time plasma shape control. In Section II, we compare the Jacobians of emulated shape targets with those obtained from finite differences of exact GS solutions to quantify the accuracy of the emulated VCs, and the target displacements obtained by re-solving GS equilibria after the VCs are applied. In Section III, we analyse the effect of vessel currents and provide procedures to account for their effect in shaping the plasma. We use emulators trained on large synthetic libraries of equilibria, generated using a Markov-Chain Monte Carlo method [11], with the initial conditions seeded near real MAST-U [Mega-Ampère Spherical Tokamak Upgrade, 12] equilibria.

A. Notation

This work is rather dense on specific notation from tokamak plasma physics, so we provide this short section as a reference. A collection of currents $\{I_c\}_{c=1,\dots,n_c}$ will also be denoted by a vector $\underline{I}_{(c)}$, where the subscript (c) may indicate actively-controlled PF coils ($c = a$) or passive vessel structures ($c = v$). The regression slopes in Section III are written as $b^{(c,\tau)}$ to distinguish them from the “plasma beta” ratios of thermodynamic and magnetic pressures. The MAST-U machine description and coil nomenclatures are provided by [11, 12]. Following [13], throughout this paper the flux function $\psi(R, Z)$ is defined from the vertical magnetic field B_Z as

$$\psi(R, Z) = \int_0^R B_Z(R', Z) R' dR' \quad (1)$$

with radial and vertical coordinates measured from the tokamak axis and from the midplane respectively (see Figure 1).

II. VALIDATION OF EMULATOR JACOBIANS

In this work, the input parameters considered for the emulators are the coil currents and plasma current density profile coefficients. The targets of interest are the inner and outer radii at the midplane (R_{in} , R_{out}), the coordinates of lower the X-point (R_X, Z_X), and the radial position of the lower divertor “nose gap” (R_{gap}) and strike-point (R_s), as shown in Figure 1.

A. Data and emulators

In view of new machines, and to include configurations not yet explored, large synthetic datasets of plasma equilibria are necessary. A random combination of input parameters is very

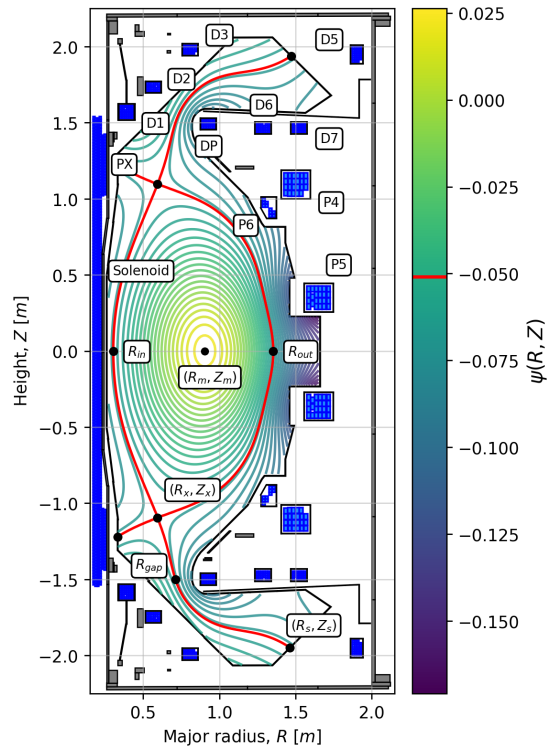


Fig. 1. A poloidal cross-section of a plasma equilibrium from MAST-U [shot 45456 at $t = 0.72$ s, resolved with FreeGSNKE 14, 15], delimited by the last closed flux surface (in red). Labels mark the basic shape control targets, PF and Ohmic coils are in blue and passive vessel structures are in gray. The contours of total ψ are plotted only within the “plasma domain” bounded by the inner wall structures.

unlikely to result in configurations with closed flux surfaces or desirable properties (e.g. divertor leg strike points or lower X-point positions). To achieve this, we build upon previous work [11]. Starting from reasonable parameter choices, a Markov-Chain Monte Carlo (MCMC) random walk algorithm sequentially samples the input parameters, promoting equilibrium configurations with desirable properties. The random walk enables faster convergence of the GS solver, and the parameter step sizes are adaptively adjusted.

We use FreeGSNKE [14, 15], to obtain GS equilibria for the chosen combinations of plasma parameters and PF coil currents. While [11] built entirely synthetic libraries, we start from snapshots of MAST-U experiments as initial seeds for each MCMC. We obtain $\approx 1.8 \times 10^6$ equilibria with robustly computed targets and a separatrix entirely contained in the vessel, which include configurations encountered in MAST-U campaigns so far and extend to yet unseen configurations. From this, we separate a *holdout set* of 3.5×10^5 equilibria close to the MAST-U MCMC seeds, which is never used to train or evaluate the shape emulators.

Following [11], the emulators are fully-connected, feed-forward neural networks (FNNs), because they fulfil universal approximation theorems and are compositions of functions with defined and non-trivial gradients almost everywhere. We train the FNNs to reproduce shape control targets versus PF coil currents, plasma current, internal inductance and poloidal beta [see e.g. 2, 13, for definitions]. The emulators

are trained to minimise the mean-absolute deviation over a training set, plus an L^2 regularisation loss whose amplitude is a hyperparameter to be tuned [11]. We draw a random subset of the cleaned data minus the holdout, and separate a random 20% test set. We split the remainder into an 80% training and 20% validating set whenever a choice of hyperparameters is made, and implement early stopping and learning-rate shrinkage by monitoring the FNN loss (mean absolute error) on the validation set. We examined both a Thompson sampler and an annealing sampler to tune the FNN hyperparameters. We run training and tuning experiments for different choices of dataset size, up to 10^6 . Optimal models have $\approx 5\text{--}10$ layers and 100–200 nodes per layer. Aggregating the five best FNNs achieves 1% relative residual scatter ($\sqrt{1 - R^2}$) and $<0.03\%$ relative bias in the target predictions. The results in this work are reported for a Leaky Rectified Linear Unit activation function, although we have also trained emulators with Exponential Linear Unit and sigmoid activations, trained on 1.6×10^5 equilibria.

B. Jacobians and VC displacements

While FNNs are universal approximations of L^p functions, there is no guarantee that their derivatives are also a good fit to the target function derivatives. The FNNs are trained on the shape targets instead of their Jacobians, as a lower-dimensional target space allows for simpler FNN architectures and therefore more lenient weight regularisation. We quantify the accuracy of the emulators by computing Jacobians and their pseudo-inverse VCs around a random subset of 380 equilibria in the holdout set defined above. We use these VCs to request 5 mm displacements in each of the considered shape targets: we apply the relevant VC to the PF coil currents and resolve the GS problem to obtain the actual displacements. We compare such realised displacements with those resulting from application of the FreeGSNKE VCs, obtained via finite differences.

Each row in Figure 2 refers to a desired displacement in each of the shape targets, and shows the histograms of the actual displacements in all targets. Different coloured histograms correspond to including different subsets of targets when computing the VCs. Perfect decoupling of the targets by the VCs would correspond to a peak at 1 on the diagonal panels and at 0 elsewhere. While the accuracy of the numerical VCs is superior (typically percent level), the VCs from the emulators also display, overall, good performances (typically 5–10%). This is especially the case on the ‘core’ shape targets (R_{in} , R_{out} , R_X , Z_X), where the performance is often comparable to the finite difference VCs. When compared to the finite difference VCs, the performance is poorer for requested shifts in R_s , although the actual spread in that case is only at percent level. Requesting VCs that can decouple both R_{gap} and R_s appears more challenging and would warrant further exploration. It should also be noted that calculation of ‘exact’ finite difference VCs is not without its challenges. In absence of auto-differentiable GS solvers, finite differences need to be carefully sized to result in effective VCs. The results relating to finite difference

VCs presented here are computed by referring to a relative variation of 0.002 in the plasma current density distribution. We have found that, typically, finite difference VCs computed by referring to the relative variation in the targets themselves, are less accurate.

III. SHAPING CURRENTS

Besides the PF coils, whose currents are actively controlled via the power supplies, other toroidally symmetric *passive* conductors are present all around the plasma, e.g. vessel metals and graphite tiles in the divertor. As the PF currents and plasma current distribution change through a shot, they can induce significant currents in the passive structures which in turn make a non-negligible contribution to ψ and therefore the plasma shape. Typically, *shaping currents* are defined that seek to reabsorb the passive structure contribution, i.e. currents that would be needed in the PF coils (alone) to produce the same flux ψ as the full set of currents in the PF coils and passive structures. This approach is used when virtual circuits are pre-computed for new experiments using reconstructed equilibria from a previous shot. When such VCs are applied in the control loop, the requested currents are in fact the shaping currents.

A. Offline inference of shaping currents

The active PF coil currents $\{I_a\}_{a=1,\dots,n_a}$ and passive vessel currents $\{I_v\}_{v=1,\dots,n_v}$ produce the *tokamak flux*

$$\psi_{\text{tok}}(R, Z) = \sum_{c \in a \oplus v} \mathcal{G}(R, Z; R_c, Z_c) I_c. \quad (2)$$

Over a computational grid of points (R_i, Z_j) , the Green functions \mathcal{G} generate matrices of known coefficients $G_{i,j}^c = \mathcal{G}(R_i, Z_j; R_c, Z_c)$, so the shaping currents can be inferred via ordinary linear regression

$$\underline{I}_{(s)} = (\mathbf{G}^T \mathbf{G})^\dagger \mathbf{G}^T \underline{\psi}_{\text{tok}}, \quad (3)$$

where $\dim(\underline{I}_{(s)}) = n_a$ and the dagger denotes the pseudo-inverse. This can be calculated, for each equilibrium in the dataset, using only the active coil Green function matrix elements. The regression is carried out over (R_i, Z_j) points within the limiter/wall only (see caption of Fig. 1).

The validation of this model is performed on ≈ 2700 snapshots across 21 different MAST-U shots. We restrict the inference and validation to snapshots from the ‘flat-top’ phases (where plasma current is roughly constant and maximal for the discharge), since transient currents in passive structures tend to be stronger in the ramp-up/down phases, which are not usually controlled with active feedback loops.

The inferred shaping currents can differ from the PF coil currents with statistical significance across the 21 shots, as shown in Figure 3. Based on the R^2 metric, the shaping current model explains more than 98% of variability of ψ_{tok} in all validation cases, with a residual scatter $\sqrt{1 - R^2}$ below 0.01 for the majority of validation snapshots, as shown in Figure 4. This result means that, at least for MAST-U shots, the equilibria can indeed be parameterised by a set of

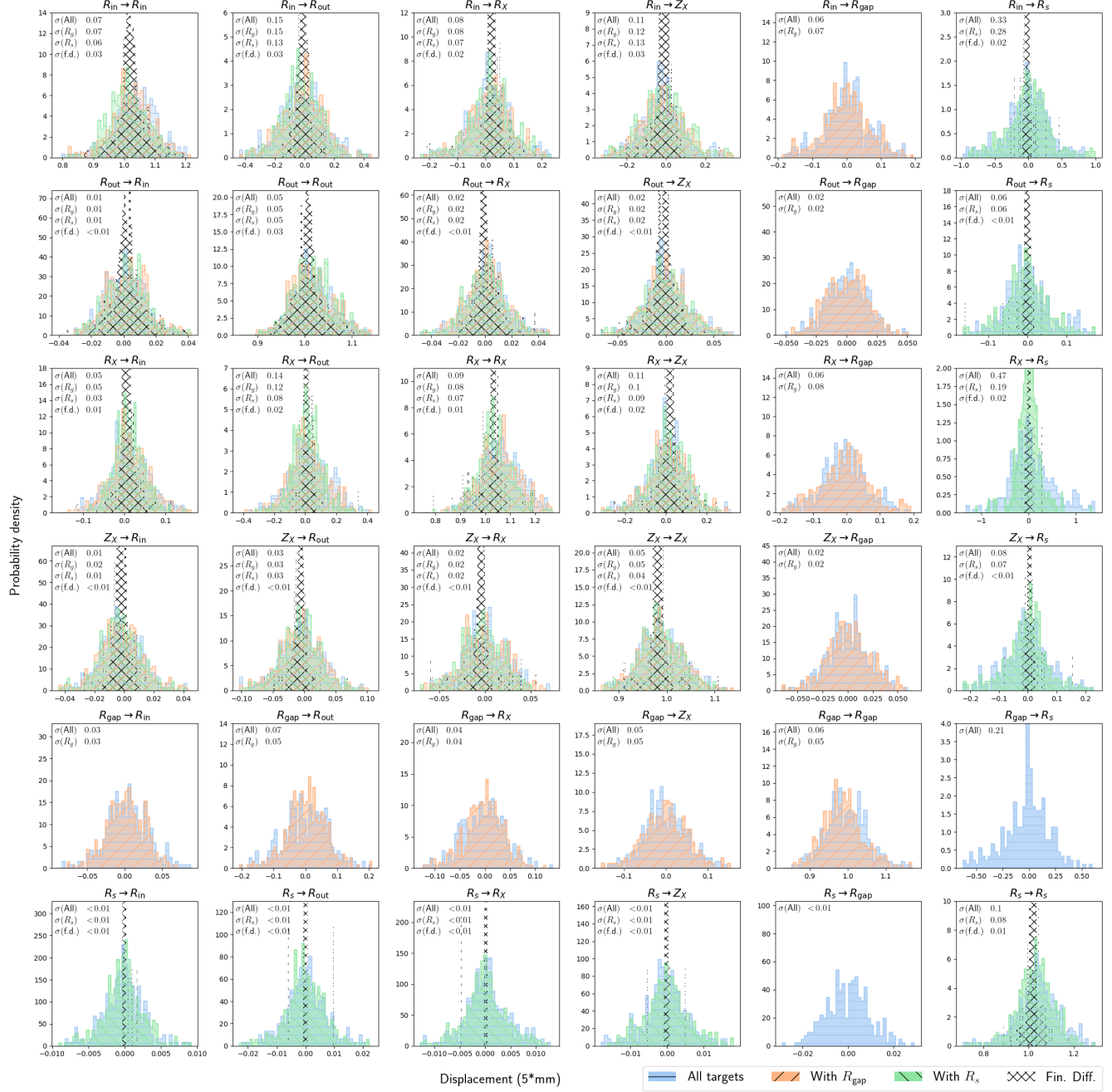


Fig. 2. Displacements in shape targets (R_{in} , R_{out} , R_X , Z_X , R_{gap} , R_s) across 380 equilibria in the holdout set after applying the VCs from the emulator-based Jacobians (coloured histograms) or the FreeGSNKE finite-difference Jacobians (black), followed by solving the GS equation. All displacements are in units of the requested 5 mm shift in shape targets. Axis ranges are proportional to the standard deviations in the targets. The reported standard deviations are for VCs applied to the core shape targets (R_{in} , R_{out} , R_X , Z_X) combined with R_{gap} or R_s or both.

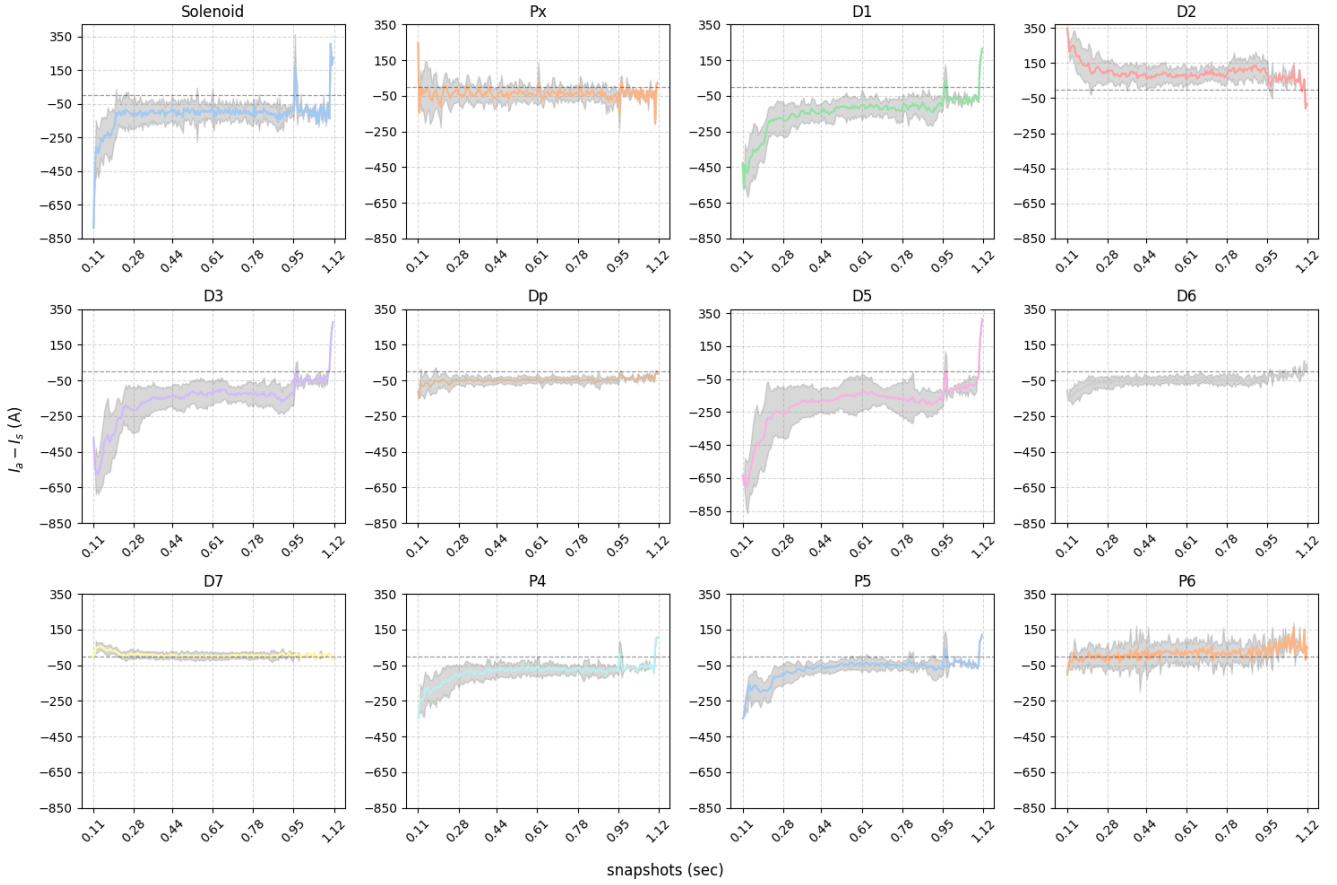


Fig. 3. Differences between shaping currents and measured coil currents for 21 MAST-U shots. Each plot shows $\mu \pm \sigma$ of the difference across all shots for all snapshots in the corresponding active current. These differences can be fit with simple regressions that result in few-Ampères residuals.

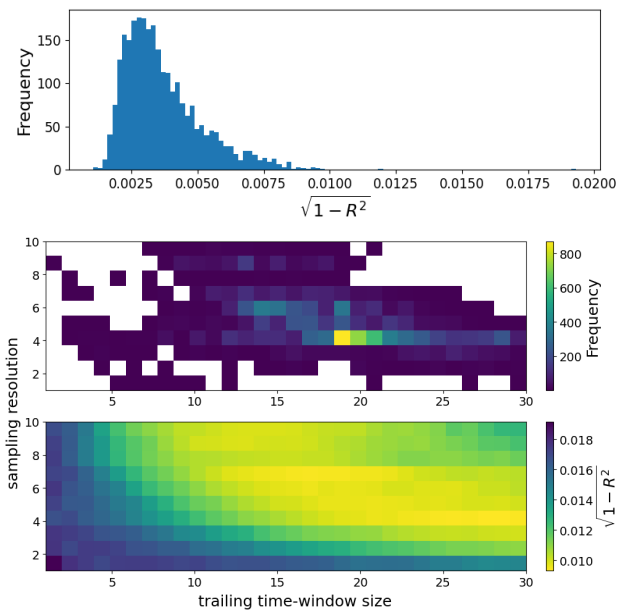


Fig. 4. Distribution of relative residual scatter in $\psi_{tok}(R_i, Z_j)$ from fits with shaping currents for 21 MAST-U shots. *Middle*: Occurrences when each setup of regressors for the online inference (eq. 4) was the best solution, over 10^4 runs with randomised train/test splits. *Bottom*: Performance of the online inference of shaping currents as linear combinations across different setups for one of the random train/test splits.

effective currents at the PF coil locations, albeit with different values than those measured in real time.

This “offline inference” requires a sufficiently accurate ψ_{tok} reconstruction, which is not necessarily performed in real time. The MAST-U equilibria in our dataset have a sampling rate of 5 ms, whereas the active currents are measured every 0.6 ms.

B. Online inference of shaping currents

Due to the inductive coupling of active and passive PF structures, we may then seek a linear surrogate of the shaping currents using a trailing time-window of active current measurements in conjunction with the plasma current I_p . These are integrated quantities that can be measured or inferred with sub-millisecond cadence. In particular, we examine linear regressions of the form

$$I_s(t) - I_a(t) \sim \sum_{a',\tau} b^{(a',\tau)} I_{a'}(t - \tau) + b^{(p,\tau)} I_p(t - \tau), \quad (4)$$

with $s, a = 1, \dots, n_a$, where τ denotes some chosen time-lag in a trailing window, and the matrix $\mathbf{B} = [b^{(a,\tau)} | b^{(p,\tau)}]$ is to be found. Here, \mathbf{B} is posited to be the same across all shots, i.e. an inherent property of the tokamak.

Different choices for the window size and sampling resolution of past readings (at $t - \tau$) can affect the quality of the inference. We train the regressions on 11 MAST-U shots,

using a different set of 10 more shots as a validation set. The results in Figure 4 show that the optimal setup has a sampling resolution of 4 time steps in the active currents and a trailing window of $\tau = 19$ previous snapshots, corresponding to $\sqrt{1 - R^2} = 0.015$ on the validation set. This setup was by far the most frequently chosen solution in a set of 10^4 random train/test splits.

IV. DISCUSSION

Different methods from machine learning can provide fast and smooth policies for real-time control. Emulation of control targets can provide explainable and robust control policies, but like pre-computed lookup matrices its accuracy is limited by the approximations required for real-time applicability, in particular, that of sufficiently small models on reasonably low-dimensional input and target spaces.

The tests of Jacobian and VC displacement accuracy in Section II indicate that VCs appropriate to different equilibria can, in principle, be predicted by differentiable emulators trained on the shape targets (typical accuracy of 5-10% in the resulting displacements). Training the emulators on the shape targets allows for more compact architectures that are less prone to overfitting and can provide low enough latency (a few ms for $10^5 - 10^6$ parameters). If higher accuracies are deemed necessary, the emulator models may be fine-tuned on the finite difference VCs themselves.

During feedback control, the voltage requests on power supplies are proportional to the difference between desired and measured shape targets – as well as their numerical derivatives and integrals over a trailing time window. These differences are parametrised in terms of currents because they are directly related to voltages through the circuit equations and can be more intuitively constrained to remain within operational limits. Currents induced in the vessel can be non-negligible, so the PF current corrections are better interpreted in terms of the above-defined shaping currents, which can best reproduce the same flux as the full set of PF coils and passive structures. The shaping currents can be computed offline, from post-experiment equilibrium reconstructions, or as linear combinations of PF coil currents over a sliding time window, with percent-level accuracy and statistically negligible residuals. Since the PF coil currents can be measured with sub-millisecond cadence, the shaping currents can also be computed and adjusted every millisecond. This is a substantial improvement over existing approaches that use virtual circuit lookup tables pre-computed for phases of the experiment that are separated by hundreds of milliseconds.

REFERENCES

[1] de Tommasi, G., et al., “XSC Tools: A Software Suite for Tokamak Plasma Shape Control Design and Validation”, *IEEE Transactions on Plasma Science*, vol. 35, no. 3, IEEE, pp. 709–723, 2007. doi:10.1109/TPS.2007.896989.

[2] Ariola, M., et al., “Integrated Plasma Shape and Boundary Flux Control on JET Tokamak”, *Fusion Science and Technology*, vol. 53, no. 3, pp. 789–805, 2008. doi:10.13182/FST08-A1735.

[3] Ambrosino, G., et al., “Plasma Strike-Point Sweeping on JET Tokamak With the eXtreme Shape Controller”, *IEEE Transactions on Plasma Science*, vol. 36, no. 3, IEEE, pp. 834–840, 2008. doi:10.1109/TPS.2008.922920.

[4] Ariola, M., Ambrosino, G., Lister, J. B., Pironti, A., Villone, F., and Vyas, P., “A Modern Plasma Controller Tested on the TCV Tokamak”, *Fusion Technology*, vol. 36, no. 2, pp. 126–138, 1999. doi:10.13182/FST99-A97.

[5] McArdle, G., Pangione, L., and Kochan, M., “The MAST Upgrade plasma control system”, *Fusion Engineering and Design*, vol. 159, Art. no. 111764, 2020. doi:10.1016/j.fusengdes.2020.111764.

[6] Seo, J., “Feedforward beta control in the KSTAR tokamak by deep reinforcement learning”, *Nuclear Fusion*, vol. 61, no. 10, Art. no. 106010, IOP, 2021. doi:10.1088/1741-4326/ac121b.

[7] Degrave, J., et al., “Magnetic control of tokamak plasmas through deep reinforcement learning”, *Nature*, vol. 602, no. 7897, pp. 414–419, 2022. doi:10.1038/s41586-021-04301-9.

[8] Zhang, Y. C., Wang, S., Yuan, Q. P., Xiao, B. J., and Huang, Y., “Real-time feedback control of β_p based on deep reinforcement learning on EAST”, *Plasma Physics and Controlled Fusion*, vol. 66, no. 5, Art. no. 055014, IOP, 2024. doi:10.1088/1361-6587/ad3749.

[9] Tracey, B. D., et al., “Towards practical reinforcement learning for tokamak magnetic control”, *Fusion Engineering and Design*, vol. 200, Art. no. 114161, 2024. doi:10.1016/j.fusengdes.2024.114161.

[10] Wai, J. T., Boyer, M. D., and Kolemen, E., “Neural net modeling of equilibria in NSTX-U”, *Nuclear Fusion*, vol. 62, no. 8, Art. no. 086042, IOP, 2022. doi:10.1088/1741-4326/ac77e6.

[11] Agnello, A., et al., “Emulation techniques for scenario and classical control design of tokamak plasmas”, *Physics of Plasmas*, vol. 31, no. 4, Art. no. 043901, AIP, 2024. doi:10.1063/5.0187822.

[12] Fishpool, G., et al., “MAST-upgrade divertor facility and assessing performance of long-legged divertors”, *Journal of Nuclear Materials*, vol. 438, pp. S356–S359, 2013. doi:10.1016/j.jnucmat.2013.01.067.

[13] Freidberg, J. P., *Plasma Physics and Fusion Energy*, Cambridge, UK: Cambridge University Press, 2008.

[14] Amorisco, N. C., Agnello, A., Holt, G., Mars, M., Buchanan, J., and Pamela, S., “FreeGSNKE: A Python-based dynamic free-boundary toroidal plasma equilibrium solver”, *Physics of Plasmas*, vol. 31, no. 4, Art. no. 042517, AIP, 2024. doi:10.1063/5.0188467.

[15] Pentland, K., et al., “Validation of the static forward Grad-Shafranov equilibrium solvers in FreeGSNKE and Fiesta using EFIT++ reconstructions from MAST-U”, *Physica Scripta*, vol. 100, no. 2, Art. no. 025608, IOP, 2025. doi:10.1088/1402-4896/ada192.